NeuroImage: Clinical 35 (2022) 103089

Contents lists available at ScienceDirect

NeuroImage: Clinical

journal homepage: www.elsevier.com/locate/ynicl

Cognitive control inhibition networks in adulthood are impaired by early iron deficiency in infancy

Algarín Cecilia [a,*], Peirano Patricio [a], Chen Donna [b], Hafiz Rakibul [b], Reyes Sussanne [a], Lozoff Betsy [c], Biswal Bharat [b]

[a] Sleep and Functional Neurobiology Laboratory, Institute of Nutrition and Food Technology, University of Chile, Chile
[b] Department of Biomedical Engineering, New Jersey Institute of Technology, University Heights, Newark, NJ, United States
[c] Department of Pediatrics and Environmental Health Sciences, University of Michigan, Ann Arbor, MI, United States

ARTICLE INFO

Keywords:
Iron deficiency anemia in infancy
Early adulthood
Cognitive inhibition
rs-fMRI

ABSTRACT

Iron deficiency, a common form of micronutrient deficiency, primarily affects children and women. The principal cause of iron deficiency is undernutrition in low-income countries and malnutrition in middle to upper income regions. Iron is a key element for myelin production, neuronal metabolism, and dopamine functions. Iron deficiency in early life can alter brain development and exert long-lasting effects. Control inhibition is an executive function that involves several brain regions, including the prefrontal cortex and caudate and subthalamic nuclei. Dopamine is the prevalent neurotransmitter underlying cognitive inhibition. We followed cohort study participants who had iron deficiency anemia in infancy as well non-anemic controls. At 22 years of age, the participants were subjected to functional magnetic resonance imaging (fMRI) to evaluate the correlation between functional connectivity and performance on an inhibitory cognitive task (Go/No-Go). We hypothesized that former iron deficient anemic (FIDA) participants demonstrate less strength in functional connectivity compared with controls (C). There were not significant group differences in the behavioral results in terms of accuracy and response time. A continuous covariate interaction analysis of functional connectivity and the Go/No-Go scores demonstrated significant differences between the FIDA and C groups. The FIDA participants demonstrated less strength in connectivity in brain regions related to control inhibition, including the medial temporal lobe, impairment in the integration of the default mode network (indicating decreased attention and alertness), and an increase in connectivity in posterior brain areas, all of which suggest slower circuitry maturation. The results support the hypothesis that FIDA young adults show differences in the connectivity of networks related to executive functions. These differences could increase their vulnerability to develop cognitive dysfunctions or mental disorders in adulthood.

1. Introduction

Despite economic growth in developing countries, iron deficiency (ID) remains common, affecting a substantial portion of the world population (Levi et al., 2016). Even in the United States, ID affects approximately 15% of 1–2-year-old children, and 11% of adolescents girls (Powers and Buchanan, 2019). Iron is a key element for myelin production, neuronal metabolism, and dopamine function (Vallée, 2017). After birth, the importance of iron during distinctive periods has been demonstrated (Georgieff, 2017), and an understanding of the underlying mechanisms related to cognitive and behavioral effects continues to evolve. Iron is essential for oligodendrocytes to produce myelin during development (Yeung et al., 2014). ID in infancy also alters dopaminergic receptors, reducing the activity of dopamine transporters and potentially altering the cognitive circuits where dopamine is the most important neurotransmitter (Pino et al., 2017; Radlowski and Johnson, 2013). Thus, early in life, ID could affect brain circuitry due to altered myelination or dopamine neurotransmission. Even if infants are appropriately treated with iron, effects may be observed later in life. We have found evidence of a variety of disruptions in neurofunctioning in children who had iron deficiency anemia (IDA) in infancy: longer latencies in auditory and visual responses (suggesting myelin compromise; (Algarín et al., 2013), alterations in memory recognition (Congdon et al., 2012), disruption of executive functions (EFs; Algarín et al.,

* Corresponding author at: El Líbano 5524, Macul 7830490, Región Metropolitana, Santiago, Chile.
E-mail address: calgarin@inta.uchile.cl (A. Cecilia).

https://doi.org/10.1016/j.nicl.2022.103089
Received 8 April 2022; Received in revised form 14 June 2022; Accepted 16 June 2022
Available online 21 June 2022

2013), and altered motor activity (Angulo-Barroso et al., 2013). However, it is still unknown whether former iron deficient anemic (FIDA) individuals reach their peers over time or whether the neurodevelopmental derailment affects daily cognitive performance and hinders the achievement of goals in life. Only recently have the long-term effects of IDA during infancy been studied with magnetic resonance imaging (MRI) techniques (Algarín et al., 2017). Using resting state functional MRI (rs-fMRI), WE showed that FIDA individuals presented differences in connectivity with respect to controls (C).

Resting state functional connectivity has shown how brain activity is organized in time and space, and it is expressed by the networks that connect different regions that accomplish different functions (Biswal et al., 1995, 2010; Mennes et al., 2010). Studies have shown a relation between structural and functional connectivity organization (Bullmore and Sporns, 2009; Dopper et al., 2014; Kundu et al., 2013), suggesting that structural cerebral connections are the basis of functional connectivity (Greicius et al., 2009; Uddin et al., 2011). The NW represents several anatomical regions (Jin et al., 2018) that are linked to white matter connections (Van Den Heuvel and Pol, 2011). Studies using the rs-fMRI approach have shown the role of network connectivity in cognitive control (Luna et al., 2001), and small fluctuations in active flow in the resting state during cognitive processing could influence the final performance of a determined task (Ito et al., 2017). Functional connectivity network studies have shown a different way to map the brain functions in the normal state as well as in the presence of behavioral disorders and complex psychiatric disease (Jung et al., 2014; Lynch et al., 2013).

EFs are superior brain functions considered indispensable for normal development and efficient life skills (avoid aggressive impulse, wait for one's turn, etc.) and include inhibitory control, working memory, the capacity to make decisions, and cognitive flexibility (Rothbart and Posner, 2005). fMRI studies using the Go/No Go task show development differences in activation, specifically greater dorsal and lateral prefrontal activation in children relative to adults (Mostofsky and Simmonds, 2008).On the other hand, rs-fMRI studies have characterized around 20 functional brain networks, several of which would support cognitive control function. The cingulo-opercular network and posterior parietal network support several EFs. An adequate balance between these two networks is needed to protect against cognitive failure (Marek et al., 2015). Gonzalez Alam et al. (2018) showed that individuals with stronger connectivity in the inhibitory areas activated during the Go/No-Go task had better behavioral performance.

In summary, disruption of neurodevelopmental processes by nutritional deficiency early in life may cause long-lasting changes to tissue structures, metabolic regulation, and neurophysiological functions. We hypothesized that the FIDA group shows weaker connectivity in those networks related to inhibitory cognitive control compared with the C group.

2. Methods

2.1. Participants

The sample belongs to a cohort project that has been performed in Chile since 1990, funded by a National Institutes of Health (NIH) grant entitled "Neuromaturational delays in iron deficient anemic infants". The inclusion criteria were term, uncomplicated vaginal birth, and no acute or chronic health problems. Iron status in infancy was defined as follows: anemia, venous hemoglobin (HB) $\leq$ 100 g/L at 6 months and $<$ 110 g/L at 12 or 18 months; ID $\geq$ 2 of 3 iron measures in the deficient range (mean cell volume $<$ 70 fl, erythrocyte protoporphyrin $\geq$ 1.77 μM red blood cells [100 μg/dL], serum ferritin $<$ 12 ng/mL). IDA infants were identified at 6, 12, or 18 months; non-anemic infants of the same age (HB $>$ 115 g/L) were randomly selected to generate the C group. All infants with IDA were treated with ferrous sulfate (15 mg iron/day at 6 months, 30 mg/day thereafter until 12 months). To reduce the chances of developing IDA, infants in the C group were also treated with iron. Both groups had similar background characteristics including sex; social economic status (SES, based on the Graffar questionnaire); maternal age, education, and depressive symptoms; and absence of the father. Participants with IDA in infancy and the C group were invited to perform neurophysiological studies during infancy, childhood, adolescence, and young adulthood. Participants from both groups no longer had ID or IDA.

In young adulthood, all participants who had accepted neuropsychological testing were invited to have MRI studies. Participants provided signed informed consent according to the norms for Human Experimentation, Code of Ethics of the World Medical Association (Declaration of Helsinki, 1995). The original and follow-up protocols were approved and reviewed annually by the Institutional Review Boards of the University of Michigan, Ann Arbor, and the Institute of Nutrition and Food Technology, University of Chile, Santiago.

2.2. Go/No-Go task

We used the Go/No-Go paradigm to evaluate cognitive motor inhibition (Algarín et al., 2013). To perform the task, participants were seated in front of a computer and asked to press a button, as fast as possible, in response to the presentation of all letters (target stimuli) except for the letter "X'' (non-target stimuli), while trying to avoid mistakes. For each trial, a single letter appeared in the center of the computer screen. The stimuli were uppercase letters in white typeface against a dark blue background. The letters were 1.8 cm ($1^1/_8$ inches) in height and 1.5 cm (½ inch) in width and subtended a visual angle of 2.65° and 1.19°. Each trial lasted 800 ms: 100 ms of pre-trial stimulus, 300 ms of letter presentation, and 400 ms of post-trial stimulus. There were two blocks of trials: Block 1 consisted of 50 trials containing 100% target stimuli or Go trials (Block1_Go). These trials primed participants to respond to the target stimulus. Block 2 had 400 trials containing 50% target stimuli or Go trials (Block 2_Go) and 50% non-target stimuli or No-Go trials (Block2_No-Go) corresponding to the response inhibition condition (Algarín et al., 2013). The parameters analyzed were the percentage of correct responses (accuracy) in Block1_Go, Block2_Go, and Block 2_No-Go, and response time (RT, the time measured from when the stimulus appeared on the screen to when the subject pressed the button) in Block1_Go and Block2_Go. The results were correlated with functional estimates of rs-fMRI.

2.3. Imaging

2.3.1. Data acquisition

MRI data were acquired using a Siemens 3 T Skyra MRI scanner (Siemens Healthcare, Erlangen, Germany) at Clinica Alemana in Santiago, Chile. The following parameters were used: 40 axial slices, thickness/gap = 3/3 mm, FOV = 896 mm × 840 mm, 244 volumes. TR/TE = 2500/20 ms, FA = 80°, in-plane resolution = 64 × 64. rs-fMRI data were processed using custom MATLAB-, AFNI-, and FSL-based scripts following the thousand functional connectome pipeline (Biswal et al., 2010). First, DICOM files were converted to NIFTI images. For all but two subjects, 244 volumes were kept, and the remaining volumes were discarded. For two subjects, 20 of 244 volumes were excluded due to high motion.

Pre-processing was performed using the Statistical Parametric Mapping 12 toolbox (https://www.fil.ion.ucl.ac.uk/spm/) within the MATLAB environment (MathWorks Inc., Natick, MA, USA). However, after normalization, some modules from the Functional Software Library (FSL, FMRIB Analysis Group, Oxford, UK) and Analysis of Functional Neuroimages (AFNI, nimh.nih.gov) were used for speed optimization, filtering, and smoothing the data as part of an inhouse custom-made parallel processing script. The first four time points were removed to reduce transient scanner artifacts. The six steps are explained in detail below.

Step 1: Motion correction for head movement using a least-squares approach and six-parameter (rigid body) spatial transformation with respect to the mean image of the scan was performed. A total of 85 subjects (38C, 47 FIDA) were used for the following steps after eliminating 2 subjects with excessive head motion determined using framewise displacement. A subject was eliminated if either the maximum framewise translation or rotation exceeded 1.5 mm, or the mean framewise displacement of translation or rotation exceeded 0.2 mm. *Step 2*: Co-registration of the mean functional image of each subject to their corresponding anatomical image was performed. *Step 3*: Segmentation of anatomical images into gray matter, white matter (WM), and cerebrospinal fluid (CSF) tissue probability maps was conducted. *Step 4*: Spatial normalization to the MNI space was done using deformation field vector obtained from the segmentation (in *Step 3*) of each subject and resampling to isotropic voxel size of $3 \times 3 \times 3$ mm^3. *Step 5*: Regression of the first five principal components of WM and CSF time series extracted from voxels of WM and CSF probability maps thresholded > 0.98, along with other nuisance head motion noise using Friston's 24-parameter model (6 head motion parameters + 6 previous time point motion parameters + 12 corresponding quadratic parameters). *Step 6*: Temporal filtering between 0.01 and 0.1 Hz and then, finally, spatial smoothing was conducted on the data using a Gaussian kernel of 8 mm full width at half maximum (FWHM).

Our aim was to investigate local activity and functional connectivity at the whole brain and network levels, respectively. Therefore, the analysis section was divided into two parts. The first part addressed the local activity measures and the second part investigated whole brain functional connectivity. The goal was to look at group-level interactions, differences between the C and FIDA groups for every single behavioral measure for each of the three task categories after regressing out age and sex as covariates of no interest.

2.3.2. Local activity analysis: Whole brain level

To investigate local brain activity and to characterize spontaneous fluctuations of BOLD signals at the frequency level, AFNI's "3dRSFC" (Resting State Functional Connectivity) was used to generate resting state measures. The regional homogeneity (ReHo) maps were generated using AFNI's "3dReHo." These functional segregation methods provide local information based on rs-fMRI activity within specific brain regions. The generated maps were spatially smoothed with 8 mm FWHM, converted to Z-score maps, and concatenated group wise according to a GLM design. ReHo analysis was performed on a voxel-by-voxel basis on the whole brain. Kendall's coefficient of concordance (KCC) of time series of a given voxel with those of its neighbor was calculated (Kendall and Gibbons, 1990). Voxels were considered to be neighbors if their corners were touching. A larger ReHo value indicated higher regional synchronization. To assess interactions, the mean KCC score of each cluster was found separately for every subject in the C and FIDA groups and regressed against the behavioral score of the percentage of correct responses for Block 2_Go. KCC scores from the C group demonstrated a positive correlation with higher accuracy scores. The GLM was generated and the "randomize" module was used to run 10,000 permutations to generate a null distribution and to achieve familywise error–corrected p-values. Masks were generated from the group mean of all scans and subjects using AFNI's "3dAutomask." This mask was fed to the "randomize" module to generate both corrected and uncorrected voxel-wise p-value maps. The "-tfce" option was also used to perform threshold free cluster enhancement.

2.3.3. Randomize output interpretation

The first step was to observe the corrected "tfce" (1 – p) maps of each resting state measure at two contrast levels of interaction, namely [C > FIDA] and [FIDA > C]. If any voxel survived the threshold of thr(1 – p) > 0.95, it would be significant. However, the voxel-wise uncorrected "p-stat" maps were also used as an input to AFNI's 3FWHMx with the auto-correlation function option "-acf" to generate the a, b, and c parameters. These parameters were fed into "3dClustSim" to estimate probability maps within a range of alpha and p-values in order to observe possible lower thresholds that may have meaningful interpretation. The (1 – p)-value maps were used with a threshold of thr(1 – p) > 0.95 to look for significant clusters in AFNI GUI using "Clusterize.".

The concatenated maps were fed into a GLM of each covariate of interest from each behavioral task condition. The interaction model was based on a GLM prepared in FSL. The interaction model indicates if the slope of C versus a covariate of interest is greater than the slope of FIDA versus the same covariate of interest.

2.3.4. Functional connectivity analysis – Network-level dual regression

The first step of this analysis includes performing an independent component analysis (ICA) incorporating FSL's "melodic" module. The time series of both the C and FIDA groups were concatenated to generate distinct resting state networks (RSNs). The group level Z score maps generated from "melodic" were used to run a dual regression to generate individual subject level maps for both C and FIDA participants. The Z-score maps of each RSN for each individual subject per group were concatenated. This generated one 4D file for each network that includes all C and FIDA subjects. An unpaired two-sample *t*-test with continuous covariate interaction was run.

3. Results

The Go/No-Go task was performed by 87 participants at 22 years of age: 40 (46%) in the C group and 47 (54%) in the FIDA group. The rs-fMRI sample size was 85, because data for two C participants were rejected due to excessive head motion. There were no group differences in background characteristics such as SES, maternal education, and intelligence quotient (IQ) in childhood. As expected, there were differences between the groups in iron measures at infancy (Table 1).

3.1. Behavioral results in the Go/No-Go task

3.1.1. Accuracy

Participants performed better in Block 1_Go trials than in Block 2_Go and Block 2_No-Go trials ($p < 0.01$ for both comparisons). There were no differences between the C and FIDA groups (mean [standard error of the mean] 92.1% [0.9%] vs. 91.5% [0.8%]).

3.1.2. RT

Overall, participants had a faster RT for Block 1_Go trials than for Block 2_Go trials [311 ± 4.8 ms vs. 406 ± 4.8 ms; $p = 0.001$). There were no differences between the FIDA and C groups. The results for each group are presented in Table 2.

Table 1
Sociodemographic characteristics and iron status.

	FIDA	C	p value
Sex (%)	M (60)	M (42)	0.07
Age (years)	22.2 ± 1.1	22.6 ± 1.5	0.29
Intelligence quotient (10 years of age)	92.6 ± 11.3	93.1.2 ± 9.7	0.82
Socioeconomic status	34.5 ± 13.4	34.8 ± 5.5	0.08
Mother's education (years)	9.3 ± 2.5	9.8 ± 2.8	0.39
Mother's age (at birth)	26.70 ± 6.5	24.7 ± 5.7	0.14
Iron status			
Hematocrit (6 months) %	32.9 ± 1.8	36.1 ± 2.3	< 0.001
Hemoglobin (6 months) 100 g/L	103.2 ± 8.1	122.8 ± 9.1	< 0.001
Ferritin (6 months) ng/mL	7.1 ± 7.7	19.2 ± 14.9	< 0.001

Values are expressed as mean ± standard deviation and were evaluated with Student's *t*-test.
C: control; FIDA: former iron deficient anemic.

Table 2
Accuracy and response time for the Go/No-Go task by condition and group.

	FIDA	C	p value
Accuracy, % correct responses			
Block 1_Go	97.3 ± 0.2	97.6 ± 0.3	0.10
Block 2_Go	93.6 ± 0.5	93.7 ± 0.7	0.86
Block 2_No-Go	83.6 ± 0.9	85.7 ± 0.9	0.56
Response time (ms)			
Block 1_Go	307.7 ± 45.3	316.8 ± 55.6	0.41
Block 2_Go	409.7 ± 37.1	403.7 ± 29.5	0.41

Values are expressed as mean ± standard error and were evaluated with Student's *t*-test.
C: Control; FIDA: former iron deficient anemic.

3.2. rs-fMRI results

3.2.1. Local brain activity Analysis: ReHo

As mentioned in section 2, the interaction model shows whether the slope of C versus a covariate of interest is greater than the slope of FIDA versus the same covariate of interest. Following this model, continuous covariate interaction of ReHo only revealed a significant difference between the C and FIDA groups in Block 2_Go accuracy. The C group showed five distinct clusters and higher interaction with accuracy compared with the FIDA group. Cluster 1 consisted of 179 voxels with peak t-scores located in the right thalamus (RTh; Table 3). Similarly, clusters 2, 3, 4 and 5 peaked in the right superior temporal gyrus (RSTG), the right paracentral lobule (RPaCL), the left posterior cingulate gyrus (LPCG), and the right posterior cingulate gyrus (RPCG) (Fig. 1).

In summary, for the C group accuracy showed a higher interaction compared with the FIDA group. The interaction model revealed that the slope of C in Block 2_Go accuracy was greater than the slope of FIDA.

3.2.2. Functional connectivity analysis: Network level

Similar non-parametric analysis at the network level revealed group differences in the medial temporal network (MTN), the dorsal attention network (DAN), the executive control network (EXEC), and the default mode network (DMN). The C group demonstrated greater interaction between functional connectivity and behavioral measures in MTN for Block1_Go and Block 2_Go conditions relative to the FIDA group (Table 4). There were three clusters in the grey matter for the Block 1_Go condition with peak t-scores in the left insula (LIns), the left superior temporal gyrus (LSTG), and the right middle temporal gyrus (RMTG) (Fig. 2a). For the Block 2_Go condition, there were two clusters with peak t-scores in the left middle temporal gyrus (LMTG) and the LIns (Fig. 2b).

On the other hand, compared with the C group, the FIDA group showed higher interaction in the DAN for the Block 2_Go condition (Table 5). There was a single cluster peaking at the right lingual gyrus (RLiG) (Fig. 3). In terms of RT for the Block 2_Go condition, compared with the C group, the FIDA group showed higher interaction for the EXEC and DMN networks.

Table 3
Cluster details from continuous covariate interaction of regional homogeneity and functional connectivity with accuracy in Block 2_Go (C > FIDA).

Anatomical location	Cluster number	Voxel extension	MNI coordinates			Peak t-score
			x	y	z	
Right thalamus	1	179	12	24	9	3.93
Right superior temporal gyrus	2	96	27	36	9	10.91
Right paracentral lobule	3	59	6	27	45	13.155
Left posterior cingulate gyrus	4	49	39	24	33	16.046
Right posterior cingulate gyrus	5	25	6	27	45	25.584

C: controls; FIDA: former iron deficient anemic.

4. Discussion

At 22 years of age, the FIDA and C participants had similar behavioral results when they performed the Go/No-Go task. However, there were differences in the interaction between the behavioral responses and neural networks displayed for each group. These findings may indicate that they use different brain strategies to perform this motor inhibition task. A lack of group differences on behavioral task performance together with differences in rs-fMRI has been interpreted as an indication of irregular development of brain connections (Moeller et al., 2016).

We observed a higher correlation between resting state brain activity and cognitive test scores for the C compared with the FIDA group in cortical and subcortical regions. Specifically, the thalamus is a key structure for cognitive control and has extensive connectivity with cerebral cortex (Cole et al., 2010). Steiner et al. (2020) showed that the thalamus-cortical circuit becomes stronger with age until young adulthood, with a positive correlation with cognitive performance. Studies with multiple-demand tasks have shown greater connectivity in subcortical regions including the thalamus and caudate nucleus independent of the stimulus type (perception, working memory, and suppression of the preponderant stimulus) (Gonzalez Alam et al., 2018), reinforcing the strong association with the inhibitory system.

The C group had a significant RTh cluster, whereas the FIDA group did not, suggesting that the FIDA participants had not developed the usual subcortical-cortical circuits to successfully perform an inhibitory cognitive task, instead developing other strategies that could be less efficient. Another relevant result is the laterality preference represented by the increased connectivity in the RTh in the C compared with the FIDA group. Several investigators have reported decreased connectivity of the RTh and its connections in psychiatry conditions (Bhikram et al., 2020; Damoiseaux and Greicius, 2009; Dopper et al., 2014). The FIDA participants showed a similar finding, which could indicate greater vulnerability for developing behavioral dysfunctions.

Non-parametric analysis at the network level revealed differences in the MTN. Compared with the FIDA participants, the C participants had a greater positive correlation between accuracy and connectivity. Areas surrounding the medial temporal lobe (MTL) are related to several cognitive actions; the peripheral region appears to process modality and task specifics, and the central core handles abstract information (Ho et al., 2019). Reinhart and Nguyen (2019) showed that subjects with impaired memory presented decreased connectivity between the MTL and the prefrontal cortex. Along the same lines, Ho et al. (2019) reported that subjects who were able to maintain focus during a task had greater connectivity between MTL and other regions of DMN and the fronto-parietal network. The MTL is also involved in the flexibility capacity of neural processing (Davis et al., 2017). Thus, the MTN is involved in cognitive inhibition as well as the capacity to find an alternative response. Our findings showing lesser connectivity in the MTN of the FIDA participants suggest that they may have impairments in cognitive inhibition.

The C group also showed greater connectivity in the LIns. Insular regions have been related to the alertness state, specifically being prepared to respond (Sadaghiani and D'Esposito, 2015). The decreased correlation between accuracy and connectivity in the LIns in the FIDA group suggests impaired attention and decreased alertness, which place the individual at a disadvantage to perform a task.

It is interesting that the MTL is one of the brain regions with less heritability (Blokland et al., 2012). This is more susceptible to be affected by environment factors, such as early ID.

Our analysis of accuracy responses also showed that the FIDA group had greater connectivity than the C group in the DAN region, particularly in the RLiG. It has been shown that in tasks that require motor

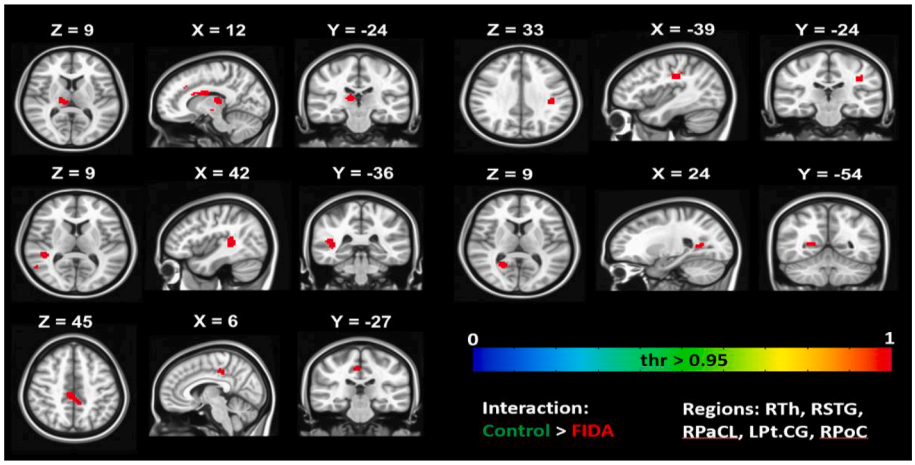

Fig. 1. Regional homogeneity brain region clusters demonstrated significantly higher interaction for control (C) compared with former iron deficient anemic (FIDA) participants in Block 2_Go accuracy scores. LPtCG: left posterior cingulate gyrus; RPaCL: right paracentral; RPoC: right posterior cingulate; RSTG: right superior temporal gyrus; Rth: right thalamus. Red indicates regions with significance.

Table 4
Functional connectivity analysis: Medial temporal network interaction (C > FIDA).

Behavior response	Anatomical location	Voxel extension	MNI coordinates			Peak t-score
			x	y	z	
Block 1_Go accuracy	LSTG	15	−60	−33	18	7.775
Block 1_Go accuracy	RMTG	14	57	−63	−3	11.89
Block 2_Go accuracy	LMTG	406	−48	−12	−24	5.014
Block 2_Go accuracy	LIG	68	−39	−18	−6	7.317

C: control; FIDA: former iron deficient anemic; LIG: left lingual gyrus; LMTG: left medial temporal gyrus; LSTG: left superior temporal gyrus; RMTG: right medial temporal gyrus.

inhibition, the salient and DAN present increase connectivity associated with the NW involved in cognitive inhibition (Hsu et al., 2020) and are implicated in the top-down control (Vossel et al., 2014).

It is well known that the period between late adolescence and young adulthood is critical for the development of more refined EFs and concurs with a decrease in synapsis and an increase in dopamine neurotransmitters in the prefrontal cortex. These changes would allow for the formation of specialized circuitry in response to the interaction between genetic and environmental factors (Petanjek et al., 2011). Any variation in development could produce changes in connectivity, inducing establishment and remodeling within neuronal circuits. A subtle change in these evolving processes could contribute to psychiatric disorders (Penzes et al., 2011). A decrease in the lingual surface area has been associated with the severity of the symptoms in young depressed adults (Couvy-Duchesne et al., 2018; Jung et al., 2014). An rs-fMRI study compared three groups of patients with diagnoses of major depressive disorder (MDD), anxiety disorders, and MDD plus anxiety disorders

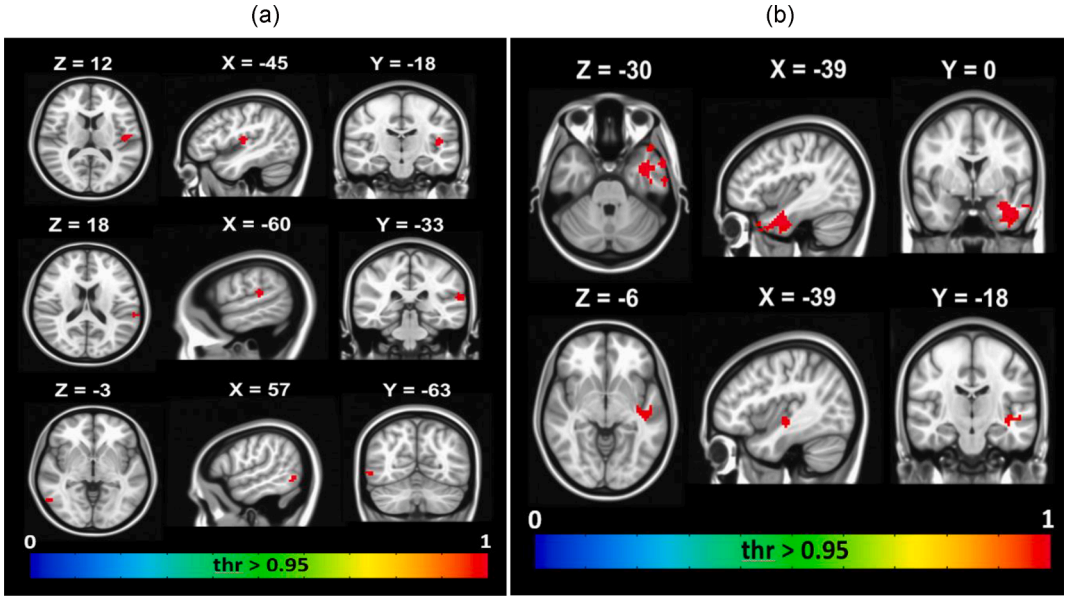

Fig. 2. (a) Brain regions in which the control (C) compared with the former iron deficient anemic (FIDA) groups demonstrated significantly higher interaction between Block 1_Go accuracy scores and functional connectivity of the medial temporal network. (b) Brain regions in which the C compared with the FIDA group demonstrated significantly higher interaction between Block 2_Go accuracy scores and functional connectivity of the medial temporal network. Red indicates regions with significance.

Table 5
Functional connectivity analysis: Network interactions (FIDA > C).

Network	Behavior response	Anatomical location	Voxel extension	MNI coordinates			Peak t-score
				x	y	z	
DAN	Block 2_Go Accuracy	RLIG	24	18	−81	−3	4.263
EXECUTIVE	Block 2_No Go RT	LCG	23	21	−81	−6	−2.425
DMN	Block 2_No Go RT	RACG	76	0	39	21	4.106

C: control; DAN: dorsal attention network; DMN: default mode network; EXECUTIVE: executive network; FIDA: former iron deficient anemic; LCG: left cingulate gyrus; RACG: right anterior cingulate gyrus; RLIG: right lingual gyrus.

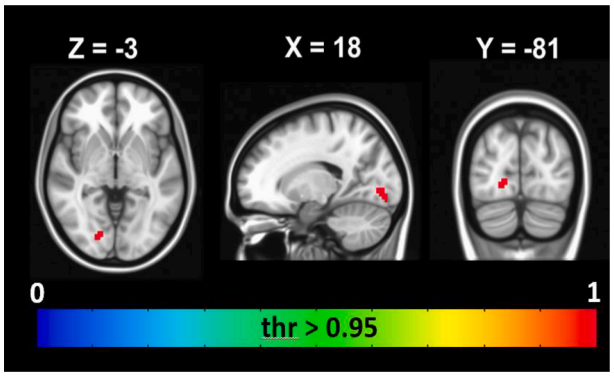

Fig. 3. Brain regions in which the former iron deficient anemic (FIDA) compared with the control (C) group demonstrated significantly higher interaction between Block 2_Go accuracy scores and functional connectivity of the dorsal attention network. An unpaired two-sample *t*-test with continuous covariate interaction was run. Red indicates regions with significance.

(Pannekoek et al., 2015). The most consistent finding was increased connectivity in the limbic network and a cluster containing the bilateral precuneus, the intracalcarine cortex, the lingual gyrus, and the posterior cingulate. Greater connectivity in the RLiG of the C but not the FIDA group suggests a lag in DAN development during adolescence and young adulthood.

In terms of RT for the Block 2_Go condition, the FIDA group showed an interaction for the DMN network not seen in the C group. The DMN is involved in rest activities related to introspection, thought wandering, and future planning, among others (Greicius et al., 2009; Raichle et al., 2001). Studies have associated RT behavioral responses with the degree of negative correlation among the DMN and the networks involved in an specific task (Barber et al., 2015; Fassbender et al., 2009; Kelly et al., 2008). Studies have shown that tasks with repeated responses produce instability, which promotes decoupling of the DMN and longer RTs (Barber et al., 2017). Spreng and Grady (2010) proposed that under conditions with greater complexity for the subject, the DMN participates in the process along with the task positive region, with a consequent misaligned function. Thus, the positive correlation between RT and DMN connectivity in the FIDA group could correspond to decoupling of the DMN secondary to instability or co-participation along the positive task. We argue that in daily-life activities, alterations in FIDA participants would contribute to decreased performance and may inform understanding of disorders involving inattention and delayed responses.

Several studies have demonstrated that reduced availability of D2/D3 receptors is associated with decreased DMN connectivity, worse task performance, and weaker functional connectivity with other networks (Nagano-Saito et al., 2017; Nour et al., 2019). ID has been associated with dopaminergic dysfunction either by abnormal D2 receptor signaling (Erikson et al., 2001; Matak et al., 2016; Youdim et al., 1989) or by its role as cofactor for tyrosine hydroxylase, an enzyme that catalyzes the rate-limiting step of dopamine synthesis (Pino et al., 2017).

The DMN has a strong correlation with functions related to social interaction: self-regulation or the ability for self-inspection. Disruptions of the DMN have been implicated in several behavioral dysfunctions, including psychiatric diseases. Weaker and unsteady connectivity between the DMN and brain regions required for EF activity would predispose alcohol or drug users to decreased awareness of negative consequences (Zhang and Volkow, 2019). DMN alterations have been observed in individuals with MDD (Wise et al., 2017), schizophrenia (Tang et al., 2013), and attention-deficit hyperactivity disorder (ADHD) (Kelly et al., 2008), and have been proposed as a robust non-invasive biomarker for brain pathology (Biswal et al., 2010).

Although the findings are consistent with previous results that we have published at other ages and tasks, the present study has some limitations. This was a cross-sectional study, which precludes inferences regarding causality. The MRI exam could not be performed at the same time in all subjects, because they were working and had little free time. Therefore, some tests could have been performed when the participant was more tired or even sleepy, which could interfere with the predominance of connectivity networks. The Go/No-Go task was designed with an extensive number of trials and reduced time to answer; however, the subjects did not present a high percentage of incorrect responses. These results prevented us from examining whether those participants with a large number of incorrect answers would have had different network behavior.

Taking into account the antecedents of our participants, the most important finding of this study is that the FIDA participants differed in connectivity in areas and networks related to cognitive inhibition. First, in the FIDA group the DMN showed weaker intrinsic connection, despite similar behavioral results in the C and FIDA groups. We speculate that the differences in the DMN could reflect the long-lasting effect of ID on myelination and formation of dopamine circuits. Even in an easy task to evaluate cognitive control inhibition such as Go/No-Go, the underlying networks to accomplish the task were different in the FIDA group and might be less efficient. Second, the only positive association that was stronger for FIDA > C was found in the DAN, and the greatest cluster was the RLiG. These results suggest a slower maturation process in FIDA participants, creating a vulnerable state or increasing the risk of triggering a genetic predisposition for mental diseases. The differences in NW connectivity could predispose one to have more difficulty in identifying and resolving conflicts in daily life, and these subjects may be more vulnerable to a mental disorder.

5. Availability of data

Due to ethical restrictions, the data have not been deposited in a database. In the informed consent that all participants signed (approved by the Institutional Review Boards of the University of Michigan, Ann Arbor, and the Institute of Nutrition and Food Technology, University of Chile), we assured them that their information would be kept confidential. The original imaging studies and the databases are deposited at the Laboratory of Sleep and Functional Neurobiology, Institute of Nutrition and Food Technology, University of Chile. All data are available for researchers who meet the criteria for access to confidential data and do not include information that could be used to identify our participants. Requests for these data may be sent to Dr. Cecilia Algarín (calgarin@inta.uchile.cl). Dr. Algarín oversees the banking of these data and will review all requests to utilize the data and images. Researchers

can also send data requests to the ethics committee of the Institute of Nutrition and Food Technology, University of Chile to comite.etica@inta.uchile.cl.

Funding

This study was supported by grants from the National Institutes of Health (NIH HD33487) and the Chilean National Fund for Scientific and Technological Development (FONDECYT; No. 11160671). The funders had no role in study design, data collection and analysis, decision to publish, or preparation of the manuscript.

CRediT authorship contribution statement

Algarín Cecilia: Conceptualization, Investigation, Methodology, Project administration, Supervision, Visualization, Writing – original draft, Writing – review & editing. **Peirano Patricio:** Conceptualization, Funding acquisition, Project administration, Writing – review & editing. **Chen Donna:** Writing – review & editing. **Hafiz Rakibul:** Data curation, Formal analysis. **Reyes Sussanne:** Funding acquisition, Project administration, Writing – review & editing. **Lozoff Betsy:** Funding acquisition, Writing – review & editing. **Biswal Bharat:** Conceptualization, Visualization, Writing – review & editing.

Acknowledgments

We would like to express our gratitude to the individuals whose participation made this study possible. We also thank technicians of the Sleep and Functional Neurobiology Laboratory of INTA, University of Chile, for their contribution during the course of this study.

References

Algarín, C., Karunakaran, K.D., Reyes, S., Morales, C., Lozoff, B., Peirano, P., Biswal, B., 2017. Differences on brain connectivity in adulthood are present in subjects with iron deficiency anemia in infancy. Front. Aging Neurosci. 9 https://doi.org/10.3389/fnagi.2017.00054.

Algarín, C., Nelson, C.A., Peirano, P., Westerlund, A., Reyes, S., Lozoff, B., 2013. Iron-deficiency anemia in infancy and poorer cognitive inhibitory control at age 10 years. Dev. Med. Child Neurol. 55, 453–458. https://doi.org/10.1111/dmcn.12118.

Angulo-Barroso, R.M., Peirano, P., Algarin, C., Kaciroti, N., Lozoff, B., 2013. Motor activity and intra-individual variability according to sleep-wake states in preschool-aged children with iron-deficiency anemia in infancy. Early Hum. Dev. 89, 1025–1031. https://doi.org/10.1016/j.earlhumdev.2013.08.014.

Barber, A.D., Caffo, B.S., Pekar, J.J., Mostofsky, S.H., 2017. Decoupling of reaction time-related default mode network activity with cognitive demand. Brain Imaging Behav. 11, 666–676. https://doi.org/10.1007/s11682-016-9543-4.

Barber, A.D., Jacobson, L.A., Wexler, J.L., Nebel, M.B., Caffo, B.S., Pekar, J.J., Mostofsky, S.H., 2015. Connectivity supporting attention in children with attention deficit hyperactivity disorder. NeuroImage Clin. 7, 68–81. https://doi.org/10.1016/j.nicl.2014.11.011.

Bhikram, T., Arnold, P., Crawley, A., Abi-Jaoude, E., Sandor, P., 2020. The functional connectivity profile of tics and obsessive-compulsive symptoms in Tourette Syndrome. J. Psychiatr. Res. 123, 128–135. https://doi.org/10.1016/j.jpsychires.2020.01.019.

Biswal, B., Zerrin Yetkin, F., Haughton, V.M., Hyde, J.S., 1995. Functional connectivity in the motor cortex of resting human brain using echo-planar mri. Magn. Reson. Med. 34, 537–541. https://doi.org/10.1002/mrm.1910340409.

Biswal, B.B., Mennes, M., Zuo, X.N., Gohel, S., Kelly, C., Smith, S.M., Beckmann, C.F., Adelstein, J.S., Buckner, R.L., Colcombe, S., Dogonowski, A.M., Ernst, M., Fair, D., Hampson, M., Hoptman, M.J., Hyde, J.S., Kiviniemi, V.J., Kötter, R., Li, S.J., Lin, C. P., Lowe, M.J., Mackay, C., Madden, D.J., Madsen, K.H., Margulies, D.S., Mayberg, H.S., McMahon, K., Monk, C.S., Mostofsky, S.H., Nagel, B.J., Pekar, J.J., Peltier, S.J., Petersen, S.E., Riedl, V., Rombouts, S.A.R.B., Rypma, B., Schlaggar, B.L., Schmidt, S., Seidler, R.D., Siegle, G.J., Sorg, C., Teng, G.J., Veijola, J., Villringer, A., Walter, M., Wang, L., Weng, X.C., Whitfield-Gabrieli, S., Williamson, P., Windischberger, C., Zang, Y.F., Zhang, H.Y., Castellanos, F.X., Milham, M.P., 2010. Toward discovery science of human brain function. Proc. Natl. Acad. Sci. U. S. A. 107, 4734–4739. https://doi.org/10.1073/pnas.0911855107.

Blokland, G.A.M., De Zubicaray, G.I., McMahon, K.L., Wright, M.J., 2012. Genetic and environmental influences on neuroimaging phenotypes: a meta-analytical perspective on twin imaging studies. Twin Res. Hum. Genet. 15, 351–371. https://doi.org/10.1017/thg.2012.11.

Bullmore, E., Sporns, O., 2009. Complex brain networks: graph theoretical analysis of structural and functional systems. Nat. Rev. Neurosci. 10, 186–198. https://doi.org/10.1038/nrn2575.

Cole, M.W., Pathak, S., Schneider, W., 2010. Identifying the brain's most globally connected regions. Neuroimage 49, 3132–3148. https://doi.org/10.1016/j.neuroimage.2009.11.001.

Congdon, E.L., Westerlund, A., Algarin, C.R., Peirano, P.D., Gregas, M., Lozoff, B., Nelson, C.A., 2012. Iron deficiency in infancy is associated with altered neural correlates of recognition memory at 10 years. J. Pediatr. 160, 1027–1033. https://doi.org/10.1016/j.jpeds.2011.12.011.

Couvy-Duchesne, B., Strike, L.T., de Zubicaray, G.I., McMahon, K.L., Thompson, P.M., Hickie, I.B., Martin, N.G., Wright, M.J., 2018. Lingual gyrus surface area is associated with anxiety-depression severity in young adults: A genetic clustering approach. eNeuro 5, ENEURO.0153-17.2017. doi: 10.1523/ENEURO.0153-17.2017.

Damoiseaux, J.S., Greicius, M.D., 2009. Greater than the sum of its parts: a review of studies combining structural connectivity and resting-state functional connectivity. Brain Struct. Funct. 213 (6), 525–533.

Davis, S.W., Stanley, M.L., Moscovitch, M., Cabeza, R., 2017. Resting-state networks do not determine cognitive function networks: a commentary on Campbell and Schacter (2016). Language, Cognition and Neuroscience 32 (6), 669–673.

Dopper, E.G.P., Rombouts, S.A.R.B., Jiskoot, L.C., Heijer, T.D., De Graaf, J.R.A., De Koning, I., Hammerschlag, A.R., Seelaar, H., Seeley, W.W., Veer, I.M., Van Buchem, M.A., Rizzu, P., Van Swieten, J.C., 2014. Structural and functional brain connectivity in presymptomatic familial frontotemporal dementia. Neurology 83, 19–26. https://doi.org/10.1212/WNL.0000000000000583.

Erikson, K.M., Jones, B.C., Hess, E.J., Zhang, Q., Beard, J.L., 2001. Iron deficiency decreases dopamine D1 and D2 receptors in rat brain. Pharmacol. Biochem. Behav. 69, 409–418. https://doi.org/10.1016/s0091-3057(01)00563-9.

Fassbender, C., Zhang, H., Buzy, W.M., Cortes, C.R., Mizuiri, D., Beckett, L., Schweitzer, J.B., 2009. A lack of default network suppression is linked to increased distractibility in ADHD. Brain Res. 1273, 114–128. https://doi.org/10.1016/j.brainres.2009.02.070.

Georgieff, M.K., 2017. Iron assessment to protect the developing brain. Am. J. Clin. Nutr. 106, 1588S–1593S. https://doi.org/10.3945/ajcn.117.155846.

Gonzalez Alam, T., Murphy, C., Smallwood, J., Jefferies, E., 2018. Meaningful inhibition: exploring the role of meaning and modality in response inhibition. Neuroimage 181, 108–119. https://doi.org/10.1016/j.neuroimage.2018.06.074.

Greicius, M.D., Supekar, K., Menon, V., Dougherty, R.F., 2009. Resting-state functional connectivity reflects structural connectivity in the default mode network. Cereb. Cortex 19, 72–78. https://doi.org/10.1093/cercor/bhn059.

Ho, N.S.P., Wang, X., Vatansever, D., Margulies, D.S., Bernhardt, B., Jefferies, E., Smallwood, J., 2019. Individual variation in patterns of task focused, and detailed, thought are uniquely associated within the architecture of the medial temporal lobe. Neuroimage 202, 116045. https://doi.org/10.1016/j.neuroimage.2019.116045.

Hsu, H.M., Yao, Z.-F., Hwang, K., Hsieh, S., Bergsland, N., 2020. Between-module functional connectivity of the salient ventral attention network and dorsal attention network is associated with motor inhibition. PLoS One 15 (12), e0242985.

Ito, T., Kulkarni, K.R., Schultz, D.H., Mill, R.D., Chen, R.H., Solomyak, L.I., Cole, M.W., 2017. Cognitive task information is transferred between brain regions via resting-state network topology. Nat. Commun. 8, 1027. https://doi.org/10.1038/s41467-017-01000-w.

Jin, F., Zheng, P., Liu, H., Guo, H., Sun, Z., 2018. Functional and anatomical connectivity-based parcellation of human cingulate cortex. Brain Behav. 8 (8), e01070.

Jung, J., Kang, J., Won, E., Nam, K., Lee, M.S., Tae, W.S., Ham, B.J., 2014. Impact of lingual gyrus volume on antidepressant response and neurocognitive functions in Major Depressive Disorder: a voxel-based morphometry study. J. Affect. Disord. 169, 179–187. https://doi.org/10.1016/j.jad.2014.08.018.

Kelly, A.M.C., Uddin, L.Q., Biswal, B.B., Castellanos, F.X., Milham, M.P., 2008. Competition between functional brain networks mediates behavioral variability. Neuroimage 39, 527–537. https://doi.org/10.1016/j.neuroimage.2007.08.008.

Kendall, M., Gibbons, J., 1990. Rank Correlation Methods, fifth ed. Edward Arnold, London.

Kundu, P., Brenowitz, N.D., Voon, V., Worbe, Y., Vértes, P.E., Inati, S.J., Saad, Z.S., Bandettini, P.A., Bullmore, E.T., 2013. Integrated strategy for improving functional connectivity mapping using multiecho fMRI. Proc. Natl. Acad. Sci. U. S. A. 110, 16187–16192. https://doi.org/10.1073/pnas.1301725110.

Levi, M., Rosselli, M., Simonetti, M., Brignoli, O., Cancian, M., Masotti, A., Pegoraro, V., Cataldo, N., Heiman, F., Chelo, M., Cricelli, I., Cricelli, C., Lapi, F., 2016. Epidemiology of iron deficiency anaemia in four European countries: a population-based study in primary care. Eur. J. Haematol. 97, 583–593. https://doi.org/10.1111/ejh.12776.

Luna, B., Thulborn, K.R., Munoz, D.P., Merriam, E.P., Garver, K.E., Minshew, N.J., Keshavan, M.S., Genovese, C.R., Eddy, W.F., Sweeney, J.A., 2001. Maturation of widely distributed brain function subserves cognitive development. Neuroimage 13, 786–793. https://doi.org/10.1006/nimg.2000.0743.

Lynch, C.J., Uddin, L.Q., Supekar, K., Khouzam, A., Phillips, J., Menon, V., 2013. Default mode network in childhood autism: Posteromedial cortex heterogeneity and relationship with social deficits. Biol. Psychiatry 74, 212–219. https://doi.org/10.1016/j.biopsych.2012.12.013.

Marek, S., Hwang, K., Foran, W., Hallquist, M.N., Luna, B., Posner, M., 2015. The contribution of network organization and integration to the development of cognitive control. PLoS Biol. 13 (12), e1002328.

Matak, P., Matak, A., Moustafa, S., Aryal, D.K., Benner, E.J., Wetsel, W., Andrews, N.C., 2016. Disrupted iron homeostasis causes dopaminergic neurodegeneration in mice. Proc. Natl. Acad. Sci. U. S. A. 113, 3428–3435. https://doi.org/10.1073/pnas.1519473113.

Mennes, M., Kelly, C., Zuo, X.-N., Di Martino, A., Biswal, B., Castellanos, F.X., Milham, M.P., 2010. Inter-individual differences in resting state functional

connectivity predict task-induced BOLD activity. Neuroimage 50, 1690–1701. https://doi.org/10.1016/j.neuroimage.2010.01.002.
Moeller, S.J., Bederson, L., Alia-Klein, N., Goldstein, R.Z., 2016. Neuroscience of inhibition for addiction medicine: from prediction of initiation to prediction of relapse. Prog. Brain Res. 223, 165–188. https://doi.org/10.1016/bs.pbr.2015.07.007.
Mostofsky, S.H., Simmonds, D.J., 2008. Response inhibition and response selection: two sides of the same coin. J. Cogn. Neurosci. 20, 751–761. https://doi.org/10.1162/jocn.2008.20500.
Nagano-Saito, A., Lissemore, J.I., Gravel, P., Leyton, M., Carbonell, F., Benkelfat, C., 2017. Posterior dopamine D2/3 receptors and brain network functional connectivity. Synapse 71, 1–13. https://doi.org/10.1002/syn.21993.
Nour, M.M., Dahoun, T., McCutcheon, R.A., Adams, R.A., Wall, M.B., Howes, O.D., 2019. Task-induced functional brain connectivity mediates the relationship between striatal D2/3 receptors and working memory. Elife 8, 1–23. https://doi.org/10.7554/eLife.45045.
Pannekoek, J.N., van der Werff, J.A., van Tol, M.J., Veltman, D.J., Aleman, A., Zitman, F. G., Rombouts, S.A., van der Wee, N.J., 2015. Investigating distinct and common abnormalities of resting-state functional connectivity in depression, anxiety, and their comorbid states. Eur. Neuropsychopharmacol. 25, 1933–1942. https://doi.org/10.1016/j.euroneuro.2015.08.002.
Penzes, P., Cahill, M.E., Jones, K.A., VanLeeuwen, J.-E., Woolfrey, K.M., 2011. Dendritic spine pathology in neuropsychiatric disorders. Nat. Neurosci. 14 (3), 285–293.
Petanjek, Z., Judaš, M., Šimić, G., Rašin, M.R., Uylings, H.B., Rakic, P., Kostović, I., 2011. Extraordinary neoteny of synaptic spines in the human prefrontal cortex. Proc. Natl. Acad. Sci. U. S. A. 108, 13281–13286. https://doi.org/10.1073/pnas.1105108108.
Pino, J.M.V., da Luz, M.H.M., Antunes, H.K.M., Giampá, S.Q. d. C., Martins, V.R., Lee, K. S., 2017. Iron-restricted diet affects brain ferritin levels, dopamine metabolism and cellular prion protein in a region-specific manner. Front. Mol. Neurosci. 10, 1–13. doi: 10.3389/fnmol.2017.00145.
Powers, J.M., Buchanan, G.R., 2019. Disorders of iron metabolism: new diagnostic and treatment approaches to iron deficiency. Hematol. Oncol. Clin. North Am. 33 (3), 393–408.
Radlowski, E.C., Johnson, R.W., 2013. Perinatal iron deficiency and neurocognitive development. Front. Hum. Neurosci. 7, 585. https://doi.org/10.3389/fnhum.2013.00585.
Raichle, M.E., MacLeod, A.M., Snyder, A.Z., Powers, W.J., Gusnard, D.A., Shulman, G.L., 2001. A default mode of brain function. Proc. Natl. Acad. Sci. U. S. A. 98, 676–682. https://doi.org/10.1073/pnas.98.2.676.
Reinhart, R.M., Nguyen, J.A., 2019. Working memory revived in older adults by synchronizing rhythmic brain circuits. Nat. Neurosci. 22, 820–827. https://doi.org/10.1038/s41593-019-0371-x.
Rothbart, M.K., Posner, M.I., 2005. Genes and experience in the development of executive attention and effortful control. New Dir. Child Adolesc. Dev. 2005 (109), 101–108.
Sadaghiani, S., D'Esposito, M., 2015. Functional characterization of the cingulo-opercular network in the maintenance of tonic alertness. Cereb. Cortex 25, 2763–2773. https://doi.org/10.1093/cercor/bhu072.
Spreng, R.N., Grady, C.L., 2010. Patterns of brain activity supporting autobiographical memory, prospection, and theory of mind, and their relationship to the default mode network. J. Cogn. Neurosci. 22, 1112–1123. https://doi.org/10.1162/jocn.2009.21282.
Steiner, L., Federspiel, A., Slavova, N., Wiest, R., Grunt, S., Steinlin, M., Everts, R., 2020. Functional topography of the thalamo-cortical system during development and its relation to cognition. Neuroimage 223, 117361.
Tang, J., Liao, Y., Song, M., Gao, J.-H., Zhou, B., Tan, C., Liu, T., Tang, Y., Chen, J., Chen, X., Zhan, W., 2013. Aberrant default mode functional connectivity in early onset schizophrenia. PLoS One 8 (7), e71061.
Uddin, L.Q., Supekar, K.S., Ryali, S., Menon, V., 2011. Dynamic reconfiguration of structural and functional connectivity across core neurocognitive brain networks with development. J. Neurosci. 31, 18578–18589. https://doi.org/10.1523/JNEUROSCI.4465-11.2011.
Vallée, L., 2017. Fer et neurodéveloppement. Arch. Pediatr. 24 (5), 5S18.
Van Den Heuvel, M.P., Pol, H.E.H., 2011. Exploring the brain network: a review on resting-state fMRI functional connectivity. Psiquiatr. Biol. doi: 10.1016/j.psiq.2011.05.001.
Vossel, S., Geng, J.J., Fink, G.R., 2014. Dorsal and ventral attention systems: Distinct neural circuits but collaborative roles. Neuroscientist 20, 150–159. https://doi.org/10.1177/1073858413494269.
Wise, T., Marwood, L., Perkins, A.M., Herane-Vives, A., Joules, R., Lythgoe, D.J., Luh, W.-M., Williams, S.C.R., Young, A.H., Cleare, A.J., Arnone, D., 2017. Instability of default mode network connectivity in major depression: a two-sample confirmation study. Transl. Psychiatry 7 (4), e1105. https://doi.org/10.1038/tp.2017.40.
Yeung, M.S.Y., Zdunek, S., Bergmann, O., Bernard, S., Salehpour, M., Alkass, K., Perl, S., Tisdale, J., Possnert, G., Brundin, L., Druid, H., Frisén, J., 2014. Dynamics of oligodendrocyte generation and myelination in the human brain. Cell 159, 766–774. https://doi.org/10.1016/j.cell.2014.10.011.
Youdim, M.B., Ben-Shachar, D., Yehuda, S., 1989. Putative biological mechanisms of the effect of iron deficiency on brain biochemistry and behavior. Am. J. Clin. Nutr. 50, 607. https://doi.org/10.1093/ajcn/50.3.607.
Zhang, R., Volkow, N.D., 2019. Brain default-mode network dysfunction in addiction. Neuroimage 200, 313–331.